doi:10.1093/brain/awp313 Brain 2010: 133; 161–171 | 161

BRAIN
A JOURNAL OF NEUROLOGY

Default network connectivity reflects the level of consciousness in non-communicative brain-damaged patients

Audrey Vanhaudenhuyse,[1,*] Quentin Noirhomme,[1,*] Luaba J.-F. Tshibanda,[1,2] Marie-Aurelie Bruno,[1] Pierre Boveroux,[1,3] Caroline Schnakers,[1] Andrea Soddu,[1] Vincent Perlbarg,[4] Didier Ledoux,[1,3] Jean-François Brichant,[3] Gustave Moonen,[5] Pierre Maquet,[1] Michael D. Greicius,[6] Steven Laureys[1,5] and Melanie Boly[1,5]

1 Coma Science Group, Cyclotron Research Centre, University of Liège, Belgium
2 Department of Radiology, CHU Sart Tilman Hospital, University of Liège, Belgium
3 Department of Anaesthesiology, CHU Sart Tilman Hospital, University of Liège, Belgium
4 Inserm, U678, Hopital La Pitié-Salpêtrière, Paris, France
5 Department of Neurology, CHU Sart Tilman Hospital, University of Liège, Belgium
6 Functional Imaging in Neuropsychiatric Disorders (FIND) Lab, Department of Neurology and Neurological Sciences, Stanford University School of Medicine, USA

*These authors contributed equally to the work.

Correspondence to: Mélanie Boly,
Coma Science Group,
Cyclotron Research Centre,
University of Liège,
Allée du 6 août, B30,
Liège, Belgium
E-mail: mboly@student.ulg.ac.be

Correspondence may also be addressed to: Steven Laureys,
Coma Science Group,
Cyclotron Research Centre,
University of Liège,
Allée du 6 août, B30,
Liège, Belgium
E-mail: steven.laureys@ulg.ac.be

The 'default network' is defined as a set of areas, encompassing posterior-cingulate/precuneus, anterior cingulate/mesiofrontal cortex and temporo-parietal junctions, that show more activity at rest than during attention-demanding tasks. Recent studies have shown that it is possible to reliably identify this network in the absence of any task, by resting state functional magnetic resonance imaging connectivity analyses in healthy volunteers. However, the functional significance of these spontaneous brain activity fluctuations remains unclear. The aim of this study was to test if the integrity of this resting-state connectivity pattern in the default network would differ in different pathological alterations of consciousness. Fourteen non-communicative brain-damaged patients and 14 healthy controls participated in the study. Connectivity was investigated using probabilistic independent component analysis, and an automated template-matching component selection approach. Connectivity in all default network areas was found to be negatively correlated with the degree of clinical consciousness impairment, ranging

Received July 17, 2009. Revised October 20, 2009. Accepted October 21, 2009

from healthy controls and locked-in syndrome to minimally conscious, vegetative then coma patients. Furthermore, precuneus connectivity was found to be significantly stronger in minimally conscious patients as compared with unconscious patients. Locked-in syndrome patient's default network connectivity was not significantly different from controls. Our results show that default network connectivity is decreased in severely brain-damaged patients, in proportion to their degree of consciousness impairment. Future prospective studies in a larger patient population are needed in order to evaluate the prognostic value of the presented methodology.

Keywords: Default mode; fMRI; coma; vegetative state; minimally conscious state

Abbreviations: CRS-R = Coma Recovery Scale-Revised; DMN = default mode network; fMRI = functional magnetic resonance imaging; PCC = posterior cingulate cortex

Introduction

In recent years, advances in emergency medicine and reanimation have considerably increased the number of patients surviving prolonged cardiac arrest or severe motor vehicle accidents (Laureys and Boly, 2008). An important proportion of these surviving patients are left with severe brain damage, leading to the presence of disorders of consciousness. Among disorders of consciousness, coma is defined by 'unarousable unresponsiveness'; and 'vegetative state' by preserved behavioural sleep–wake cycles and reflexive but not purposeful behaviours (Laureys and Boly, 2007). Minimally conscious patients, though unable to communicate, show inconsistent non-reflexive behaviours, interpreted as signs of awareness of self or environment (Giacino *et al.*, 2002). The locked-in syndrome describes patients who are awake and conscious but have no means of producing speech, limb or facial movements (American Congress of Rehabilitation Medicine, 1995). A particular problem in patients with disorders of consciousness is that the clinical diagnosis is very challenging at the bedside, and several studies have reported high rates of misdiagnosis, reaching up to 40% (Majerus *et al.*, 2005; Schnakers *et al.*, 2009). It is now increasingly recognized that diagnosing these distinct conditions correctly is critical, both for ethical reasons and in order to improve the clinical management of these patients. Indeed, several studies have shown that brain activation in response to auditory or painful stimuli is very limited when in a vegetative state, while this activation is virtually normal in patients who are minimally conscious (Boly *et al.*, 2004, 2008*a*), suggesting the possibility of residual external stimuli perception in the latter patient population. Furthermore, preliminary data show that patients in the minimally conscious state have a much better functional prognosis than patients in a vegetative state, independently of the aetiology (Giacino, 2005). These concerns raise the need for reliable paraclinical markers as a complement to the clinical assessment in differentiating patients in a vegetative state from patients in a minimally conscious state.

Over the last 8 years, increasing attention has been paid to the study of spontaneous brain activity and its significance for cognition and behaviour (Raichle, 2006). In particular, the concept of a 'default mode network (DMN) of brain function' was introduced by Raichle *et al.* (2001), after observing that a number of areas including the precuneus, bilateral temporo-parietal junctions and medial prefrontal cortex, were more active at rest than when the subjects were involved in an attention-demanding cognitive task. This network of areas, now commonly referred to as the 'DMN', has been replicably implicated in cognitive processes like 'day-dreaming' or 'mind-wandering', stimulus-independent thoughts or self-related thoughts (Laureys *et al.*, 2007; Mason *et al.*, 2007; Buckner *et al.*, 2008). Though the functional significance of the DMN remains a matter of debate, it has been suggested as a candidate for the network subserving basic functions related to consciousness (Boly *et al.*, 2008*b*; Greicius *et al.*, 2008). Studying this network in patients with disorders of consciousness is, at first glance, a very challenging undertaking, due to the highly subjective and complex cognitive functions reported to be supported by this network.

Several studies in healthy volunteers have shown the ability of resting state functional magnetic resonance imaging (fMRI) to identify structured patterns of functional connectivity among defined neuroanatomical systems reliably, including the DMN (Cavanna and Trimble, 2006; Damoiseaux *et al.*, 2006; Cavanna, 2007; Shehzad *et al.*, 2009). Of potentially major interest from the clinical point of view, is the fact that resting state fMRI connectivity studies allow the investigation of higher order cognitive networks like the DMN, without requiring the patients' collaboration. This fact is particularly important in non-communicative patients such as those with disorders of consciousness. Resting state fMRI acquisitions are also very easy to perform compared with standard task-based fMRI paradigms, and could thus have a potentially broader and faster translation into clinical practice. However, to date, the functional significance of resting state connectivity patterns remain unclear. Some authors have even questioned the value and interpretability of spontaneous brain activity fluctuations as recorded by fMRI (Morcom and Fletcher, 2007).

The aim of this study was to investigate DMN resting state fMRI connectivity in a cohort of patients with disorders of consciousness including coma, vegetative state, minimally conscious state and locked-in syndrome. We hypothesized that DMN connectivity strength would be related to the level of consciousness of non-communicative brain-damaged patients, as assessed by standardized behavioural scales. Furthermore, we expected a particularly strong link between the level of consciousness and connectivity in the precuneus, reported to be a central node in the DMN (Fransson and Marrelec, 2008), and potentially the most connected area in the brain (Hagmann *et al.*, 2008).

Methods

Patients

We compared 14 brain-injured patients (1 locked-in syndrome, 4 minimally conscious, 4 vegetative state and 5 coma patients, age range 25–77 years) to 14 age-matched healthy volunteers (age range 28–57 years). In patients, clinical examination was repeatedly performed using standardized scales [the Coma Recovery Scale-Revised (CRS-R) (Giacino *et al.*, 2004); and the Glasgow Liege scale (Born, 1988)] on the day of scanning, and in the week before and the week after. Table 1 reports demographic and clinical characteristics of the patients. Patients were scanned in an unsedated condition. The study was approved by the Ethics Committee of the Medical School of the University of Liège. Informed consent to participate to the study was obtained from the subjects themselves in the case of healthy subjects, and from the legal surrogate of the patients.

Data acquisition and analysis

In all subjects, 10 min resting state fMRI were acquired on a 1.5 T magnetic resonance scanner (Siemens, Germany). Two hundred multislice T_2^*-weighted fMRI images were obtained with a gradient echo-planar sequence using axial slice orientation (36 slices; voxel size: $3.75 \times 3.75 \times 3.6\,mm^3$; matrix size $64 \times 64 \times 36$; repetition time = 3000 ms; echo time = 30 ms; flip angle = 90°; field of view = 240 mm). Head movements were minimized using customized cushions. A T_1 magnetization prepared rapid gradient echo sequence was also acquired in the same session for coregistration with functional data. Monitoring of vital parameters (electrocardiogram, blood pressure, pulse oxymetry, end tidal carbon dioxide partial pressure and respiratory rate) was performed in patients by a senior anaesthesiologist throughout the experiment.

Data analysis was performed using Statistical Parametric Mapping-5 (www.fil.ion.ucl.ac.uk/spm) and probabilistic independent component analysis (Beckmann and Smith, 2004) as implemented in MELODIC, part of the Functional MRI of the Brain software library (FSL) (www.fmrib.ox.ac.uk/fsl). Independent component analysis is a statistical technique that separates a set of signals into independent (uncorrelated and non-Gaussian) spatio-temporal components (Beckmann and Smith, 2004). When applied to the T_2^* signal of fMRI, independent component analysis allows not only for the removal of artefacts (McKeown *et al.*, 1998; Quigley *et al.*, 2002), but also for the isolation of task-activated neural networks (McKeown *et al.*, 1998; Calhoun *et al.*, 2002), or of low-frequency neural networks during task-free or cognitively undemanding fMRI scans (Greicius *et al.*, 2004; Beckmann *et al.*, 2005; Seeley *et al.*, 2007). In a first step, functional images were re-aligned, normalized and smoothed (4 mm full width at half maximum Gaussian kernel) using Statistical Parametric Mapping-5. Independent component analysis was then performed separately for each individual scanning session (one single session was acquired per subject), after removal of low-frequency drifts (150 s high-pass filter). We allowed FSL to use a probabilistic estimation of the number of components as implemented in the probabilistic independent component analysis MELODIC framework (Beckman *et al.*, 2005; Beckman and Smith, 2005) aiming to identify the number of non-Gaussian sources in the data (and thus the optimal number of components needed to decompose the data), and attempting to avoid under- or over-fitting due to an incorrect number of sources. The best-fit component for each subject was then selected in an automated three-step process described as the 'goodness-of-fit' approach (Greicius *et al.*, 2004, 2008; Seeley *et al.*, 2007). This method allows for the unbiased selection of the component for each subject that best corresponds to the DMN. The template used in the present analysis for component selection was obtained from an independent dataset encompassing 19 healthy volunteers (age range 21–31 years) studied on another 3 T MRI scanner (see Supplementary Material for methodological details). First, because intrinsic connectivity is detected in the very low-frequency range (Cordes *et al.*, 2001), a frequency filter was applied to remove any components in which high-frequency signal (>0.1 Hz) constituted 50% or more of the power in the Fourier spectrum. Next, we obtained goodness-of-fit scores to the DMN template for the remaining low-frequency components of each subject. To do this, the template-matching procedure calculated the average *Z*-score of voxels falling within the chosen template minus the average *Z*-score of voxels outside the template and selected the component in which this difference (the goodness-of-fit) is the greatest. *Z*-scores here reflect the degree to which the time series of a given voxel correlates with the time series corresponding to the specific independent component analysis component, scaled by the standard deviation of the error term. The *Z*-score is therefore a measure of how many standard deviations the signal is from the background noise. Finally, the component with the highest goodness-of-fit score was selected as the 'best-fit' component and used in the subsequent group analysis. This template-matching procedure was performed separately for each subject. It is important to note that this approach does not alter the components to fit the template in any way, but merely scores the pre-estimated components on how well they match the template (Seeley *et al.*, 2007).

Next, all group analyses were performed on the subjects' best-fit component *Z*-score images. We used a random-effects model, estimating the error variance across subjects (Holmes and Friston, 1998), consisting of an ANOVA with the four different states of consciousness (controls, minimally conscious state, vegetative state and coma patients) as the between subjects factor. A correction for non-sphericity was applied to account for potentially unequal variance across groups. A first analysis aimed at identifying the DMN in the control population. A second analysis searched for linear:

$$\left[y = -x - \frac{1}{4}\sum_{i=0}^{3}(-i) \quad x = 0,\ldots,3\right]$$

non-linear (exponential):

$$\left[y = e^{-x} - \frac{1}{4}\sum_{i=0}^{3} e^{-i}\right]$$

and power law:

$$\left[y = (x+1)^{-1} - \frac{1}{4}\sum_{i=0}^{3}(i+1)^{-1}\right]$$

correlations between DMN connectivity and the level of consciousness (i.e. controls, minimally conscious state, vegetative state and coma). A third analysis looked for differences in DMN connectivity between minimally conscious state and unconscious (vegetative state and coma) patients, using a conjunction approach. A fourth analysis searched for a correlation between DMN connectivity and summed CRS-R scores. A supplementary multiple regression random effects analysis compared the single locked-in syndrome patient to other patient populations. In all our group level analyses, the subjects' age was added as a confounding factor. Results in controls were thresholded at $P<0.05$ corrected for false discovery rate at the whole brain level. All other analyses were thresholded at $P<0.05$

Table 1 Clinical, electrophysiological and structural imaging data of patients

	VS1	VS2	VS3	VS4	MCS1	MCS2	MCS3	MCS4	LIS
Clinical Features									
Sex (age, years)	Male (25)	Male (69)	Female (57)	Male (75)	Male (26)	Female (76)	Female (76)	Male (71)	Female (46)
Cause	Trauma	CRA	Haemorrhage	Encephalitis	Trauma	CO intoxication	Stroke	Encephalitis	Stroke
Time of fMRI (days after insult)	159	36	23	69	5 years	16	34	38	16
Outcome at 12 months	GOS 2	GOS 1	GOS 3	GOS 1	GOS 3	GOS 3	GOS 3	GOS 1	GOS 1
Breathing	Spontaneous	Spontaneous—with tube	Spontaneous	Spontaneous	Spontaneous	Spontaneous	Spontaneous	Spontaneous	Spontaneous
Paralysis/paresis	Tetraparesis	Tetraparesis	Tetraparesis	Tetraparesis	Tetraparesis	Tetraparesis	Tetrapraesis	Tetraparesis	Tetraplegia Preserved vertical occulomotricity
CRS-R									
Diagnosis at time of fMRI	VS	VS	VS	VS	MCS	MCS	MCS	MCS	LIS
Auditory function	Startle reflex	None	Startle reflex	Startle reflex	Reproducible movement to command	Startle reflex	Startle reflex	Startle reflex	Consistent movement to command
Visual function	None	None	Blink to threat	None	Visual pursuit	Visual fixation	Visual pursuit	Visual pursuit	Object recognition
Motor function	Flexion to pain	None	None	Flexion to pain	Flexion to pain	None	Automatic motor response	Flexion to pain	Flexion to pain
Oromotor/Verbal function	Oral reflexes	Oral reflexes	Oral reflexes	None	Oral reflexes	Oral reflexes	Oral reflexes	Oral reflexes	Oral reflexes
Communication	None	None	None	None	None	None	None	None	Functional/accurate
Arousal	With stimulation	With stimulation	With stimulation	Without stimulation	Without stimulation	With stimulation	Without stimulation	Without stimulation	Attention
Total score	5	2	4	4	11	5	12	9	16
EEG									
Background activity	Bilateral very slow delta and intermittent theta	Theta with intermittent diffuse delta	Delta-theta irregular	Diffuse delta activity	Low voltage theta, muscular artefacts	Symmetric theta–delta activity	Delta–theta, predominantly on the right side	Theta activity	Theta – with signs of reticular formation impairment
MRI									
Increased intensity on T_2	Diffuse axonal injury (thalamus, mesencephalon, bilateral grey matter)	Bilateral sylvian and frontal lesions	Bilateral frontoparietal lesions	Centro-protuberantial and bilateral white matter lesions	Diffuse leucoencephalopathy and cerebral atrophy Subcortical lesions in basal ganglia and thalamus	Bilateral pallidal lesions	Right frontotemporal lesion	Cerebellar peduncles lesions	Bulbo-medullar junction and cerebellar pedoncules lesions

(continued)

Table 1 Continued

	COMA1	COMA2	COMA3	COMA4	COMA5
Clinical Features					
Sex (age, years)	Female (49)	Male (34)	Male (40)	Male (48)	Female (77)
Cause	Meningioma coma post-surgery	Anoxia	CRA	Haemorrhage	Stroke
Time of fMRI (days after admission)	14	7	7	5	13
Outcome at 12 months	GOS 1	GOS 4	GOS 1	GOS 1	GOS 1
Breathing	Spontaneous	Spontaneous	Spontaneous with tube	Spontaneous	Spontaneous with tube
Paralysis/paresis	Tetraparesis	Tetraparesis	Tetraparesis	Tetraparesis	Tetraparesis
CRS-R					
Diagnosis at time of fMRI	Coma	Coma	Coma	Coma	Coma
Auditory function	None	None	None	None	Startle reflex
Visual function	None	Blink to threat	None	None	None
Motor function	Abnormal posturing	Flexion to pain	Abnormal posturing	None	Flexion to pain
Oromotor/Verbal function	None	None	None	None	Oral reflexes
Communication	None	None	None	None	None
Arousal	None	None	None	None	None
Total score	1	3	1	0	4
EEG					
Background activity	Theta–delta bilateral	Intermittent theta – delta Abundant spike-wakes and spikes	Generalized status epilepticus	Bilateral posterior theta	Generalized status epilepticus
MRI					
Increased intensity on T_2	Petroclival tumour with cavernous sinus and bulbomedullar junction invasion	None	Diffuse cortical, basal basal ganglia oedema and right capsulo-thalamic lesions	Left temporo-occipital and cerebral peduncles, tegmentum and vermis lesions	Left pulvinar and ascending reticular formation

GOS = Glasgow Outcome Scale; LIS = locked-in syndrome; MCS = minimally conscious state; VS = vegetative state.

corrected for false discovery rate in a 10 mm radius spherical small volume centred on *a priori* coordinates (all peak voxels from an independent DMN connectivity analysis in healthy controls previously published in Boly *et al.*, 2009).

Finally, we computed the power spectrum of the time course of each DMN component and compared obtained peak frequencies (i.e. the frequency with maximum power). Two-tailed permutation tests (Nichols and Holmes, 2002) looked for group differences using EEGLAB (Delorme and Makeig, 2004) implemented in MATLAB 7 (Mathworks, Natick, MA, USA) and results were thresholded for significance at $P<0.05$.

Results

In controls, the DMN could be reproducibly identified as a set of areas encompassing posterior cingulate cortex (PCC) /precuneus, temporo-parietal junction, medial prefrontal cortex, parahippocampal gyri, superior frontal sulci and thalamus (Fig. 1 and Table 2). The assessed non-linear functions showed a significant correlation between DMN connectivity strength and the level of consciousness in all the previously mentioned areas. Quasi identical results were obtained when exponential or power law contrasts were employed, whereas a less good fit was observed for the linear correlation, though linear correlation between connectivity and consciousness was significant (Table 3 and Fig. 2 show results for the exponential correlation). Clinical experience indicates that the decrease in consciousness between normal wakefulness, minimally conscious, vegetative state and coma is indeed non-linear (vegetative state patients' consciousness being closer to comatose patients' consciousness than to minimal consciousness). In all analyses, the peak area of significance for the correlation between connectivity and consciousness was found to be the PCC/precuneus. PCC/precuneus connectivity was also found to differentiate minimally conscious from unconscious patients (Table 4, Fig. 3). No brain area was found to be more present in DMN connectivity maps in unconscious compared with minimally conscious patients. No brain area could be identified as presenting a weaker connectivity in the single locked-in syndrome patient compared with controls. For illustrative purposes, the locked-in syndrome patient's data are displayed as red circles in Fig. 2, allowing comparison to controls' and patients' data.

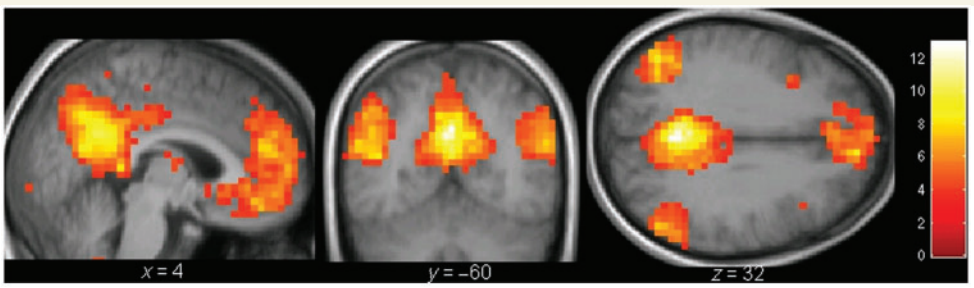

Figure 1 Default network identified in controls. Results are thresholded for display at whole brain false discovery rate corrected $P<0.01$ and rendered on the mean T_1 structural image of the controls.

Table 2 Peak voxels of the default network identified in healthy volunteers

Areas		*x*	*y*	*z*	*Z*-value	*P*-value
Posterior cingulate cortex/precuneus		−8	−52	28	6.82	<0.001
Medial prefrontal cortex		8	52	32	5.53	<0.001
Superior frontal sulcus	R	28	24	40	5.22	<0.001
	L	−20	36	48	6.05	<0.001
Temporo-parietal junction	R	52	−56	24	5.41	<0.001
	L	−48	−56	20	5.92	<0.001
Parahippocampal gyrus	L	−28	−32	−20	4.95	<0.001
Temporal cortex	R	64	−8	−24	5.44	<0.001
	L	−60	−12	−24	4.82	<0.001
Inferior frontal gyrus	R	40	24	−20	4.04	0.001
Post-central gyrus	L	−52	−16	44	3.59	0.002
Insula	L	−32	−16	8	3.00	0.013
Thalamus		−8	−8	0	2.73	0.025
Brainstem		0	−20	−24	2.71	0.026
Cerebellum	R	12	−44	−40	3.55	0.003
	L	−28	−80	−36	4.75	<0.001

P-values are corrected for false discovery rate at the whole brain level.

Table 3 Peak voxels showing an exponential correlation between default network connectivity and the level of consciousness

Areas		x	y	z	Z-value	P-value
Posterior cingulate cortex/precuneus		−8	−52	28	4.89	0.004
Medial prefrontal cortex		0	52	−20	3.52	0.025
Superior frontal sulcus	R	8	52	35	4.62	0.005
	L	−20	36	48	4.66	0.004
Temporo-parietal junction	R	60	−64	24	3.56	0.025
	L	−48	−68	24	4.10	0.009
Parahippocampal gyrus	L	−32	−20	−24	3.83	0.014
Temporal cortex	R	56	−12	−24	4.29	0.007
	L	−48	−56	20	4.26	0.007
Precentral gyrus	L	−48	−20	52	3.83	0.014
Postcentral gyrus	L	−52	−16	44	3.35	0.033
Thalamus		−24	−24	12	4.17	0.008
		8	−12	12	3.32	0.034
Brainstem		4	−24	−36	3.31	0.035
Cerebellum	R	12	−44	−40	3.90	0.012
	L	−28	−80	−36	3.46	0.028

P-values are corrected for false discovery rate for whole brain.

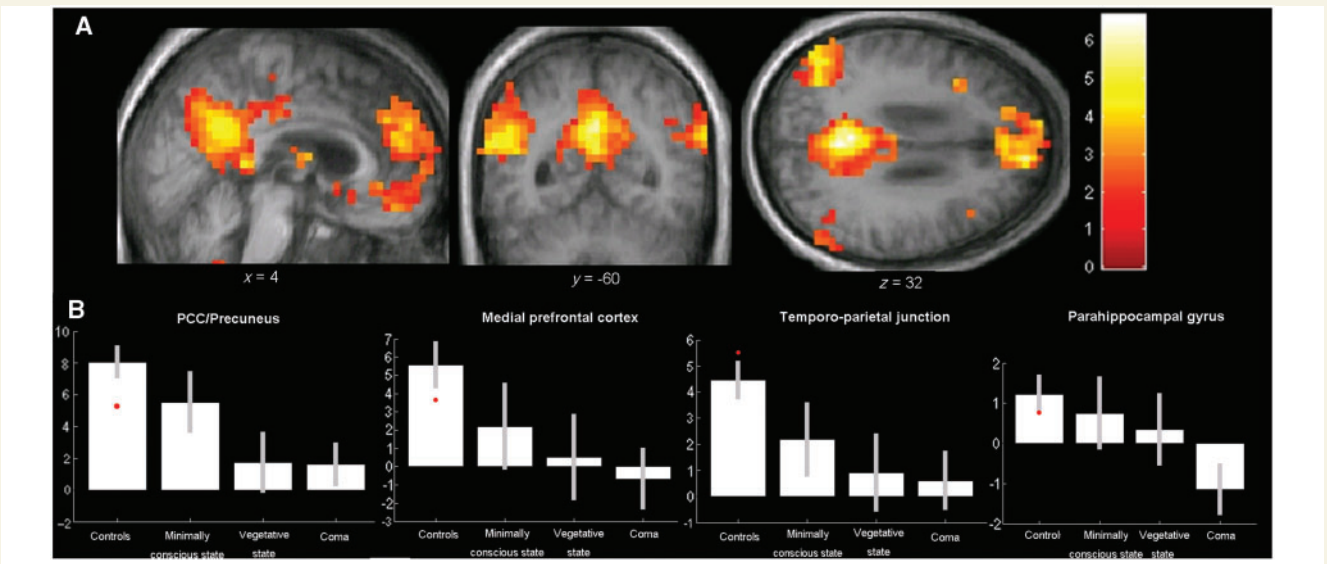

Figure 2 Default network connectivity correlates with the level of consciousness, ranging from healthy controls, to minimally conscious, vegetative then comatose patients. (**A**) Areas showing a linear correlation between default network connectivity and consciousness. Results are thresholded for display at uncorrected $P < 0.05$ and rendered on the mean T_1 structural image of the patients. (**B**) Mean *Z*-scores and 90% confidence interval for default network connectivity in PCC/precuneus, temporo-parietal junction, medial prefrontal cortex and parahippocampal gyrus across patient populations. Locked-in syndrome patient *Z*-scores are displayed for illustrative purposes as an additional red circles overlaid on control population data.

We observed a correlation between connectivity and CRS-R total scores in most of the DMN (Table 5), but results only survived correction for multiple comparisons in the medial prefrontal gyrus.

The total number of components and the proportion of variance explained by the DMN component were not significantly different in patients as compared with healthy controls [33 ± 20 (range 11–68) versus 27 ± 4 (range 21–35) components; and 4.1 ± 2.3 (range 1.2–8.7) versus 3.6 ± 0.8 (range 2.6–5.7), respectively]. Finally, the power spectrum of the DMN time courses showed a non-significant increase in peak frequency in patients as compared with healthy volunteers (mean ± SD, 0.040 ± 0.037 range 0.001–0.100 Hz versus 0.020 ± 0.013 range 0.001–0.056 Hz, respectively).

Table 4 Default network areas differentiating minimally conscious from unconscious (vegetative and coma) patients (conjunction approach)

Areas		x	y	z	Z-value	P-value
Minimally conscious state > unconscious						
Posterior cingulate cortex/precuneus		20	−48	32	3.62	0.012
Medial prefrontal cortex		−4	52	−24	1.81	0.035*
Temporo-parietal junction	R	64	−52	24	2.35	0.010*
Parahippocampal cortex	L	−32	−20	−24	2.11	0.017*
Temporal cortex	R	60	−56	28	2.35	0.010*
Thalamus		−24	−28	−12	1.75	0.040*
Brainstem		12	−16	−16	1.70	0.045*
Minimally conscious state < unconscious						
No areas could be identified						

P-values are corrected for false discovery rate in a 10 mm radius spherical small volume centred on *a priori* coordinates. *Non-corrected *P*-values.

Figure 3 Brain areas within the default network connectivity which differentiate minimally conscious patients from unconscious patients. Results are thresholded for display at uncorrected $P < 0.05$ and rendered on the mean T_1 structural image of the patients.

Table 5 Peak voxels showing a correlation between default network connectivity and the CRS-R total score

Areas		x	y	z	Z-value	P-value
Posterior cingulate cortex/precuneus		8	−32	40	2.34	0.010*
Medial frontal gyrus		−4	48	36	3.78	0.006
Superior frontal sulcus	R	16	32	40	1.70	0.044*
Parahippocampal cortex	L	−40	−4	−24	1.86	0.032*
Temporo-parietal junction	R	44	−68	48	1.89	0.030*
	L	−40	−64	52	2.07	0.019*
Temporal cortex	R	60	0	40	2.36	0.009*
	L	−60	−8	−28	1.99	0.023*
Thalamus		−16	−36	8	2.10	0.018*
Brainstem		−4	−28	−48	2.30	0.011*

P-values are corrected for false discovery rate in a 10 mm radius spherical small volume centred on *a priori* coordinates. *Non-corrected *P*-values.

Discussion

Clinical and neuroscientific relevance of a correlation between DMN connectivity and the level of consciousness

Using resting state fMRI connectivity analyses, we showed an exponential correlation between DMN connectivity integrity and the level of consciousness of brain-damaged patients ranging from controls, to minimally conscious, vegetative state then coma patients. These results suggest that, although the DMN can still be identified in unconscious patients, as in anaesthetized monkeys (Vincent *et al.*, 2007), connectivity strength within DMN could possibly be a reliable indicator of a patient's level of consciousness, differentiating unconscious patients such as those in a coma or vegetative state from minimally conscious and locked-in syndrome patients. As resting state fMRI studies are much easier to acquire in a routine clinical setting than standard fMRI paradigms, these

connectivity studies could potentially be a useful complement to bedside behavioural assessment in the evaluation of the level of consciousness of non-communicative brain-damaged patients. Note that CRS-R total scores showed a less significant fit as compared with the non-linear correlation with DMN connectivity. In our view, this is explained by the fact that the CRS-R total score was not developed to differentiate between different levels of consciousness (e.g. a minimally conscious patient may have an identical CRS-R total score as a vegetative state patient).

In addition to its potential clinical relevance, the finding that DMN connectivity strength is proportional to the level of consciousness of brain-damaged patients sheds light on the significance of spontaneous brain activity fluctuations as recorded by fMRI. Our results suggest that the strength of connectivity in resting state fMRI-identified networks could be related in a quantitative manner to the level of conscious processing in severely brain-damaged patients. These results complement previous findings showing partially preserved connectivity in states of altered consciousness like vegetative state (Boly *et al.*, 2009), light sleep (Horovitz *et al.*, 2008) or anaesthetized monkey (Vincent *et al.*, 2007). Our results are also in line with recent reports of decreased DMN connectivity in healthy volunteers during sedation (Greicius *et al.*, 2008) and deep sleep (Horovitz *et al.*, 2009). Larson-Prior *et al.* (2009), however, observed no measurable change in DMN connectivity during light sleep. Taken together, these findings suggest a two-layer view of resting state fMRI DMN connectivity: one part of the DMN connectivity would persist independently of the level of consciousness, and possibly related to underlying anatomical connectivity (Vincent *et al.*, 2007; Greicius *et al.*, 2009), and the other part being more tightly related to the presence of conscious cognitive processes. More generally, the finding of decreased DMN connectivity in proportion to impairment of consciousness is consistent with previous findings of metabolic impairment of a large frontoparietal network, encompassing main nodes of the DMN, in patients in vegetative state compared with controls, as well as in other states of clinical unconsciousness such as sleep, anaesthesia, seizures or somnambulism (Baars *et al.*, 2003; Laureys, 2005). The current results are also consistent with the so-called 'global workspace' theory of consciousness (Baars *et al.*, 2003; Dehaene and Changeux, 2005), by suggesting that higher order frontoparietal areas are likely to play a crucial role in the genesis of conscious perception. However, we should remain cautious when interpreting the functional significance of DMN connectivity measurements in terms of consciousness. More investigations on physiological (e.g. sleep and hypnotic state), pharmacological (e.g. general anaesthesia) and pathological alterations of consciousness in health and disease subjects, are awaited before a consensus can be reached on the precise functional meaning of this network.

The maximum peak of significance for a correlation between DMN connectivity and consciousness was found in the PCC/precuneus. This finding is coherent with studies showing a central role of precuneus in DMN architecture, from the functional (Fransson and Marrelec, 2008) to the structural point of view (Hagmann *et al.*, 2008). Precuneus connectivity could also reliably differentiate minimally conscious from unconscious patients, again suggesting a particularly strong relationship between the level of activity of this area and the patients' level of consciousness (Laureys *et al.*, 2004; Cavanna and Trimble, 2006). As the DMN has been suggested to be involved in 'mind-wandering' (Mason *et al.*, 2007) and self-referential processes (Cavanna and Trimble, 2006; Cavanna, 2007), our results could also imply that minimally conscious patients have a partially preserved level of self-awareness or 'day-dreaming'-like cognition or, at a minimum, have the residual functional architecture to support such complex processes. This finding stresses the importance of assessing residual cognitive functions in patients with disorders of consciousness, which could be largely underestimated at the clinical bedside.

It should be noted that while the thalamus has not been reported in all DMN connectivity studies in the literature, it has been described in papers on healthy volunteers in recent years (Fransson, 2005; De Luca *et al.*, 2006; Greicius *et al.*, 2007; Boly *et al.*, 2009). Thalamo-cortical loops have been increasingly associated with conscious perception (Laureys *et al.*, 2000; White and Alkire, 2003; Schiff *et al.*, 2007), possibly explaining our observed correlation between consciousness and thalamo-cortical DMN connectivity.

Technical issues in the study of resting state fMRI connectivity in severely brain-damaged patients

Several technical issues should be discussed in the study of connectivity in patients with altered states of consciousness. While the acquisition of resting state fMRI data is easier than standard fMRI paradigms, spontaneous blood oxygen level dependent fluctuations measures are subject to more artefactual bias than evoked data (Morcom and Fletcher, 2007). Therefore, resting state fMRI analyses should include a method for carefully separating relevant signal from artefacts present in the data. Independent component analysis is especially suited to this aim. Compared with region of interest-driven correlation analyses, independent component analysis offers the double advantage of being able to isolate cortical connectivity maps from non-neural signals (Beckmann *et al.*, 2005; Beckman and Smith, 2005; Seeley *et al.*, 2007), and of being unbiased by the selection of a seed region-of-interest for correlation analysis. Therefore, independent component analysis may allow the identification of network nodes missed by the conventional region of interest-driven analysis (Seeley *et al.*, 2007). The selection of relevant components of interest is still an issue when dealing with the outputs of independent component analysis. In a clinical framework, the use of an automated component selection approach, as used in the present analysis, is ideally required, in order to avoid subjective bias in the interpretation of data. In this study, the template used for automatic DMN component selection was issued from an independent connectivity study on a separate group of healthy volunteers, and was applied to both controls and patients. It should be noted that this methodology, classically employed in clinical studies on DMN connectivity [e.g. in dementia (Greicius *et al.*, 2004), depression (Greicius *et al.*, 2007) or epileptic patients (Zhang *et al.*, 2009)], might bias the selection towards the healthy control group. Future

work should compare the presently used 'goodness-of-fit' approach to other component selection approaches based on spatial similarity with templates, or 'fingerprinting' approaches [i.e. graphical representations of independent components in multidimensional space encompassing spatial and temporal entropy, kurtosis, one-lag auto-correlation and power contributions in different frequency bands (De Martino *et al.*, 2007)] in order to test for reliability at the individual level. Another remaining question is the relationship between structural and functional connectivity changes in non-communicative brain-damaged patients. Functional connectivity in DMN has indeed been related to underlying structural anatomy (Greicius *et al.*, 2009). Further multimodal studies should combine resting state functional MRI data with structural MRI (e.g. diffusion tensor imaging data) or high-density EEG recordings.

Conclusion

We here identified a significant correlation, at the group-level, between DMN connectivity and the level of consciousness. These results suggest that after further validation, the present methodology could potentially be rapidly translated into a routine clinical setting and bring relevant ancillary information on a patient's residual brain function to bear on their clinical evaluation. The presence of an exponential correlation between DMN connectivity and consciousness suggests that resting state fMRI could be a potentially useful paraclinical marker of the level of consciousness in non-communicative brain-damaged patients, complementing their bedside assessment. Future studies on larger samples of patients will aim at correlating resting state fMRI connectivity with prognosis and white matter damage (as assessed, for example, by diffusion tensor imaging) in individual brain-damaged patients.

Acknowledgements

The authors thank the technicians of the Department of Neuro-Radiology and the nurses of the Intensive Care and Neurology Departments of the Centre Hospitalier Universitaire of Liège for their active participation in the MRI studies in comatose patients. M.-A.B. is Research Fellow, M.B., Q.N. and C.S. are Post-doctoral Fellows, and S.L. and P.M. are Senior Research Associates at the FNRS, AV is Research Fellow at the ARC 06/11-340.

Funding

Belgian Fonds National de la Recherche Scientifique (FNRS); European Commission (Mindbridge, DISCOS, CATIA and DECODER); Mind Science Foundation; James McDonnell Foundation; French Speaking Community Concerted Research Action (ARC 06/11-340); Fondation Médicale Reine Elisabeth; NIH (NS048302 to MD.G.).

Supplementary material

Supplementary material is available at *Brain* online.

References

American Congress of Rehabilitation Medicine. Recommendations for use of uniform nomenclature pertinent to patients with severe alterations of consciousness. Arch Phys Med Rehabil 1995; 76: 205–9.

Baars BJ, Ramsoy TZ, Laureys S. Brain, conscious experience and the observing self. Trends Neurosci 2003; 26: 671–5.

Beckmann CF, DeLuca M, Devlin JT, Smith SM. Investigations into resting-state connectivity using independent component analysis. Philos Trans R Soc Lond B Biol Sci 2005; 360: 1001–13.

Beckmann CF, Smith SM. Probabilistic independent component analysis for functional magnetic resonance imaging. IEEE Trans Med Imaging 2004; 23: 137–52.

Beckmann CF, Smith SM. Tensorial extensions of independent component analysis for multisubject FMRI analysis. Neuroimage 2005; 25: 294–311.

Boly M, Faymonville ME, Peigneux P, Lambermont B, Damas P, Del Fiore G, et al. Auditory processing in severely brain injured patients: differences between the minimally conscious state and the persistent vegetative state. Arch Neurol 2004; 61: 233–8.

Boly M, Faymonville ME, Schnakers C, Peigneux P, Lambermont B, Phillips C, et al. Perception of pain in the minimally conscious state with PET activation: an observational study. Lancet Neurol 2008a; 7: 1013–20.

Boly M, Phillips C, Tshibanda L, Vanhaudenhuyse A, Schabus M, Dang-Vu TT, et al. Intrinsic brain activity in altered states of consciousness: how conscious is the default mode of brain function? Ann N Y Acad Sci 2008b; 1129: 119–29.

Boly M, Tshibanda L, Noirhomme Q, Vanhaudenhuyse A, Schnakers C, Ledoux D, et al. Functional connectivity in the default network during resting state is preserved in a vegetative but not in a brain dead patient. Hum Brain Mapp 2009; 30: 2393–400.

Born JD. The Glasgow–Liège Scale Prognostic value and evaluation of motor response and brain stem reflexes after severe head injury. Acta Neurochir 1988; 91: 9549–52.

Buckner RL, Andrews-Hanna JR, Schacter DL. The brain's default network: anatomy, function, and relevance to disease. Ann N Y Acad Sci 2008; 1124: 1–38.

Calhoun VD, Pekar JJ, McGinty VB, Adali T, Watson TD, Pearlson GD. Different activation dynamics in multiple neural systems during simulated driving. Hum Brain Mapp 2002; 16: 158–67.

Cavanna AE. The precuneus and consciousness. CNS Spectr 2007; 12: 545–52.

Cavanna AE, Trimble MR. The precuneus: a review of its functional anatomy and behavioural correlates. Brain 2006; 129 (Pt 3): 564–83.

Cordes D, Haughton VM, Arfanakis K, Carew JD, Turski PA, Moritz CH, et al. Frequencies contributing to functional connectivity in the cerebral cortex in "resting-state" data. AJNR Am J Neuroradiol 2001; 22: 1326–33.

Damoiseaux JS, Rombouts SA, Barkhof F, Scheltens P, Stam CJ, Smith SM, et al. Consistent resting-state networks across healthy subjects. Proc Natl Acad Sci USA 2006; 103: 13848–53.

Dehaene S, Changeux JP. Ongoing spontaneous activity controls access to consciousness: a neuronal model for inattentional blindness. PLoS Biol 2005; 3: e141.

Delorme A, Makeig S. EEGLAB: An open source toolbox for analysis of single-trial EEG dynamics including independent component analysis. J Neurosci Methods 2004; 134: 9–21.

De Luca M, Beckmann CF, De Stefano N, Matthews PM, Smith SM. fMRI resting state networks define distinct modes of long-distance interactions in the human brain. Neuroimage 2006; 29: 1359–67.

De Martino F, Gentile F, Esposito F, Balsi M, Di Salle, Goebel FR, et al. Classification of fMRI independent components using IC-fingerprints and support vector machine classifiers. Neuroimage 2007; 34: 177–94.

Fransson P. Spontaneous low-frequency BOLD signal fluctuations: an fMRI investigation of the resting-state default mode of brain function hypothesis. Hum Brain Mapp 2005; 26: 15–29.

Fransson P, Marrelec G. The precuneus/posterior cingulate cortex plays a pivotal role in the default mode network: evidence from a partial correlation network analysis. Neuroimage 2008; 42: 1178–84.

Giacino JT. The minimally conscious state: defining the borders of consciousness. Prog Brain Res 2005; 150: 381–95.

Giacino JT, Ashwal S, Childs N, Cranford R, Jennett B, Katz DI, et al. The minimally conscious state: definition and diagnostic criteria. Neurology 2002; 58: 349–53.

Giacino JT, Kalmar K, Whyte J. The JFK Coma Recovery Scale-Revised: measurement characteristics and diagnostic utility. Arch Phys Med Rehabil 2004; 85: 2020–9.

Greicius MD, Flores BH, Menon V, Glover GH, Solvason HB, Kenna H, et al. Resting-state functional connectivity in major depression: abnormally increased contributions from subgenual cingulate cortex and thalamus. Biol Psychiatry 2007; 62: 429–37.

Greicius MD, Kiviniemi V, Tervonen O, Vainionpaa V, Alahuhta S, Reiss AL, et al. Persistent default-mode network connectivity during light sedation. Hum Brain Mapp 2008; 29: 839–47.

Greicius MD, Srivastava G, Reiss AL, Menon V. Default-mode network activity distinguishes Alzheimer's disease from healthy aging: evidence from functional MRI. Proc Natl Acad Sci USA 2004; 101: 4637–42.

Greicius MD, Supekar K, Menon V, Dougherty RF. Resting-state functional connectivity reflects structural connectivity in the default mode network. Cereb Cortex 2009; 19: 72–8.

Hagmann P, Cammoun L, Gigandet X, Meuli R, Honey CJ, Wedeen VJ, et al. Mapping the structural core of human cerebral cortex. PLoS Biol 2008; 6: 159.

Holmes A, Friston K. Generalisability, random effects and population inference. Neuroimage 1998; 7: 754.

Horovitz SG, Braunc AR, Carrd WS, Picchionie D, Balkine TJ, Fukunagab M, et al. Decoupling of the brain's default mode network during deep sleep. Proc Natl Acad Sci USA 2009; 106: 11376–81.

Horovitz SG, Fukunaga M, de Zwart JA, van Gelderen P, Fulton SC, Balkin TJ, et al. Low frequency BOLD fluctuations during resting wakefulness and light sleep: a simultaneous EEG-fMRI study. Hum Brain Mapp 2008; 29: 671–82.

Larson-Prior LJ, Zempel JM, Nolana TS, Prior FW, Snyder AZ, Raichle MA. Cortical network functional connectivity in the descent to sleep. Proc Natl Acad Sci USA 2009; 106: 4489–94.

Laureys S. The neural correlate of (un)awareness: lessons from the vegetative state. Trends Cogn Sci 2005; 9: 556–9.

Laureys S, Boly M. What is it like to be vegetative or minimally conscious? Curr Opin Neurol 2007; 20: 609–13.

Laureys S, Boly M. The changing spectrum of coma. Nat Clin Pract Neurol 2008; 4: 544–6.

Laureys S, Faymonville ME, Moonen G, Luxen A, Maquet P. PET scanning and neuronal loss in acute vegetative state. Lancet 2000; 355: 1825–6.

Laureys S, Owen AM, Schiff ND. Brain function in coma, vegetative state, and related disorders. Lancet Neurol 2004; 3: 537–46.

Laureys S, Perrin F, Bredart S. Self-consciousness in non-communicative patients. Conscious Cogn 2007; 16: 722–41; discussion 742–25.

Majerus S, Gill-Thwaites H, Andrews K, Laureys S. Behavioral evaluation of consciousness in severe brain damage. Prog Brain Res 2005; 150: 397–413.

Mason MF, Norton MI, Van Horn JD, Wegner DM, Grafton ST, Macrae CN. Wandering minds: the default network and stimulus-independent thought. Science 2007; 315: 393–5.

McKeown MJ, Makeig S, Brown GG, Jung TP, Kindermann SS, Bell AJ, et al. Analysis of fMRI data by blind separation into independent spatial components. Hum Brain Mapp 1998; 6: 160–88.

Morcom AM, Fletcher PC. Does the brain have a baseline? Why we should be resisting a rest. Neuroimage 2007; 37:1073–82.

Nichols T, Holmes A. Nonparametric permutation tests for functional neuroimaging: a primer with examples. Hum Brain Mapp 2002; 15: 1–25.

Quigley MA, Haughton VM, Carew J, Cordes D, Moritz CH, Meyerand ME. Comparison of independent component analysis and conventional hypothesis-driven analysis for clinical functional MR image processing. AJNR Am J Neuroradiol 2002; 23: 49–58.

Raichle ME. Neuroscience. The brain's dark energy. Science 2006; 314: 1249–50.

Raichle ME, MacLeod AM, Snyder AZ, Powers WJ, Gusnard DA, Shulman GL. A default mode of brain function. Proc Natl Acad Sci USA 2001; 98: 676–82.

Schiff ND, Giacino JT, Kalmar K, Victor JD, Baker K, Gerber M, et al. Behavioural improvements with thalamic stimulation after severe traumatic brain injury. Nature 2007; 448: 600–3.

Schnakers C, Vanhaudenhuyse A, Giacino J, Ventura M, Boly M, Majerus S, et al. Diagnostic accuracy of the vegetative and minimally conscious state: clinical consensus versus standardized neurobehavioral assessment. BMC Neurology 2009; 9: 35.

Seeley WW, Menon V, Schatzberg AF, Keller J, Glover GH, Kenna H, et al. Dissociable intrinsic connectivity networks for salience processing and executive control. J Neurosci 2007; 27: 2349–56.

Shehzad Z, Kelly AM, Reiss PT, Gee DG, Gotimer K, Uddin LQ, et al. The resting brain: unconstrained yet reliable. Cereb Cortex 2009; 19: 2209–29.

Vincent JL, Patel GH, Fox MD, Snyder AZ, Baker JT, Van Essen DC, et al. Intrinsic functional architecture in the anaesthetized monkey brain. Nature 2007; 447: 83–6.

White NS, Alkire MT. Impaired thalamocortical connectivity in humans during general-anesthetic-induced unconsciousness. Neuroimage 2003; 19 (2 Pt 1): 402–11.

Zhang Z, Lu G, Zhong Y, Tan Q, Liao W, Chen Z, et al. Impaired perceptual networks in temporal lobe epilepsy revealed by resting fMRI. J Neurol 2009; 256: 1705–13.